ACS OMEGA

Open Access



http://pubs.acs.org/journal/acsodf

Article

# Immune Potentiation of PLGA Controlled-Release Vaccines for Improved Immunological Outcomes

Britteny J. Cassaidy, Brittany A. Moser, Ani Solanki, Qing Chen, Jingjing Shen, Kristen Gotsis, Zoe Lockhart, Nakisha Rutledge, Matthew G. Rosenberger, Yixiao Dong, Delaney Davis, and Aaron P. Esser- Kahn*

Cite This: *ACS Omega* 2024, 9, 11608−11614

Read Online

ACCESS | Metrics & More | Article Recommendations | Supporting Information

**ABSTRACT:** With the emergence of SARS-CoV-2 and the continued emergence of new infectious diseases, there is a need to improve and expand current vaccine technology. Controlled-release subunit vaccines provide several benefits over current vaccines on the market, including the use of less antigen and fewer boost doses. Previously, our group reported molecules that alter NF-κB signaling improved the vaccine's performance and improved adjuvant-related tolerability. In this report, we test how these immune potentiators will influence responses when included as part of a controlled-release poly(lactic-*co*-glycolic) vaccine formulation. Murine in vivo studies revealed that SN50 and honokiol improved antibody levels at early vaccine time points. Microparticles with SN50 produced strong antibody levels over a longer period compared to microparticles without SN50. The same particles also increased T-cell activity. All of the immune potentiators tested further promoted Th2 humoral responses already exhibited by the control CpG OVA microparticle formulation. Overall, under controlled-release conditions, immune potentiators enhance the existing effects of controlled-release formulations, making it a potentially beneficial additive for controlled-release vaccine formulations.

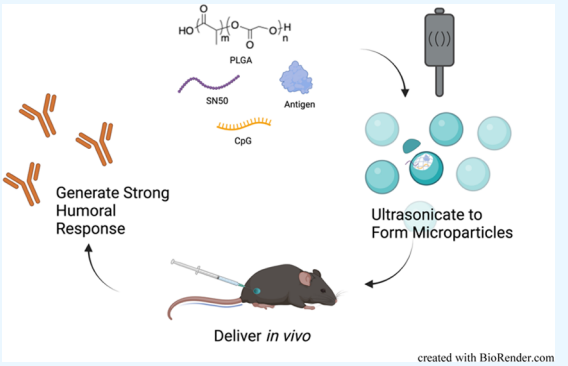


## INTRODUCTION

Particle encapsulation approaches to vaccination extend the availability of the antigen payload and adjuvant compared to the unencapsulated counterpart. This extension is the result of the steady, controlled release of particle contents and protection of the contents from cellular uptake.[1−3] Controlled-release formulations that use microparticles produce a higher and longer antibody titer than their unencapsulated and nanoparticle counterparts. Although the mechanism is not fully understood, many reports have suggested that microparticles—of sufficient size to preclude endocytosis by antigen-presenting cells (APCs)—continually release a large quantity of antigen near APCs. The increased presence of extracellular antigen promotes MHC II binding and subsequent humoral immunity.[4]

Many polymers have been used to achieve controlled release, but poly(lactic-*co*-glycolic) acid (PLGA) remains the most common, owing to its ease of formulation and degradation of its ester backbone to nontoxic components.[5] Both PLGA nanoparticles and microparticles promote prolonged antigen presentation by macrophages and dendritic cells.[6] However, a remaining challenge is that these particles still require the activation of innate pathways at the local level to stimulate an immune response. Despite producing minimal systemic inflammation, the local environment still results in cells that experience a strong innate stimulation environment. We hypothesized that immune potentiators, such as SN50, might offer the potential to enhance the local innate response further—resulting in better vaccine responses in a controlled-release system. As our group has previously demonstrated, SN50 and other potentiators alter innate pathways to promote antigen presentation through a novel mechanism.[7] In previous work, we showed that the SN50 peptide, when included with a model vaccination using CpG ODN 1826, a TLR9 agonist, successfully increased antibody response by over 2-fold compared to CpG alone, including vaccines for HIV, influenza, and dengue.[8] It has also been reported that small-molecule immune potentiators, honokiol and capsaicin, result in the same outcome.[9]

Despite the success of immune potentiator formulations in solution, the current vaccine formulation has limitations. Both SN50 and honokiol required between 200 and 500 μg to achieve their activity. The effective concentration of free

Received: November 7, 2023
Revised: January 25, 2024
Accepted: February 8, 2024
Published: February 28, 2024

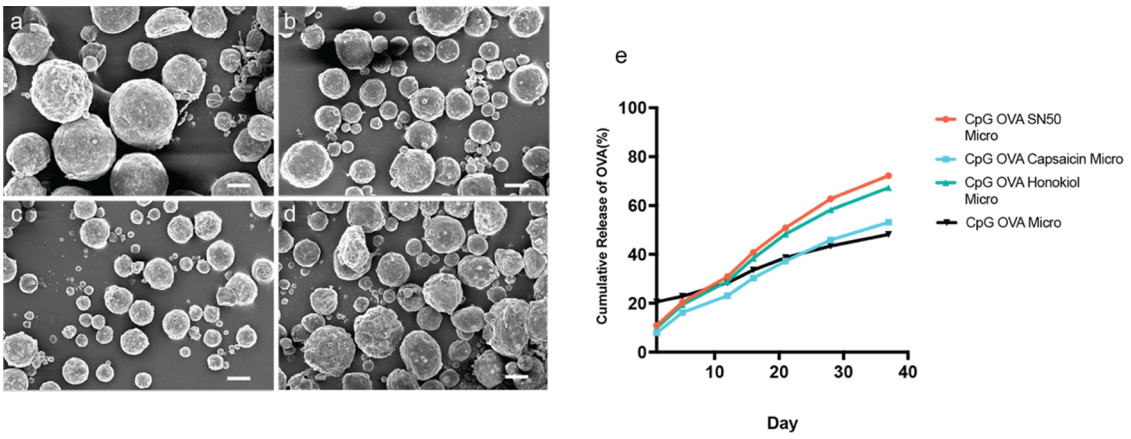


**Figure 1.** Analysis of controlled potentiator microparticles created by the double emulsion technique via SEM. (A) CpG OVA microparticles, (B) CpG OVA SN50 microparticles, (C) CpG OVA Honokiol microparticles, (D) CpG OVA Capsaicin microparticles (scale bar in all images is 10 $\mu$m). (E) In vitro release profile of microparticles containing CpG OVA Microparticles (black), CpG OVA SN50 (orange), CpG OVA Capsaicin (blue), or CpG OVA Honokiol (green) stirred in PBS at 37 °C over a 4-week period.

capsaicin resulted in side effects including hyperalgesia and temporary loss of thermal homeostasis.[9,10] With these two principles in mind, we set out to incorporate immune potentiators into controlled-release formulations.

In this study, three different immune potentiators were tested: SN50, honokiol, and capsaicin. When co-formulated with a model vaccine within the particles, each immune potentiator exhibited higher antibody levels in serum with longer durability compared to particle formulations without immune potentiators. The longer durability of the immune potentiator particle implies the need for less frequency of booster vaccinations. T cells obtained from the draining lymph node exhibited a strong MHC-II response, resulting in increased antibody responses that persisted for a longer period. In this case, it appears the potentiators simply amplify the particle response rather than alter it. These findings display that immune potentiators can be beneficial additives to sustained-release particle vaccines against infectious diseases.

## RESULTS AND DISCUSSION

The double emulsion technique was used to create sustained-release PLGA microparticles.[11] Subunit components within each particle vaccine were co-encapsulated to ensure equal exposure of agonist (CpG), antigen (ovalbumin), and immune potentiator (either SN50, honokiol, or capsaicin) in vivo. After forming the microparticles, the fidelity of the synthesis process was confirmed. Scanning electron microscopy (SEM) analysis revealed that all particles possess a sphere-like morphology with an average diameter of at least 11 $\mu$m (Figure 1A–D). The components loaded into the particles were quantified via a previously published extraction technique.[12] Most of the components encapsulated by the particles were loaded with more than 30% encapsulation efficiency (for complete details, see Table S1); however, honokiol had a low encapsulation efficiency of 0.7%. Despite the low encapsulation efficiency, testing of the particle formulation was still pursued given that PLGA controlled-release vaccines have a track record of dosing a fraction of the payload while maintaining or improving efficacy.[13−15] Of note, different particles had slightly different morphologies upon formulation with the honokiol (CpG OVA Honokiol Micro) and capsaicin (CpG OVA Capsaicin Micro) particles, each possessing enhancement of observable pore-like structures. (Figure 1A–D). These differences may be attributed to the incorporation of small molecules in contrast to the protein and peptide nature of OVA and SN50. While it is difficult to confirm the reason for these differences, we speculate that these pores might be due to the ability of small molecules to alter the solvent exchange process and thereby enlarge pore size (Figure 1A).[16,17]

The subtle differences in morphology may alter the release rate of the particles. As a result, the in vitro rate of release of the contents from the particles was measured using a standard protocol.[18] All of the particles were found to exhibit a sustained-release profile in vitro over a 40-day period (Figure 1E). However, the CpG OVA microparticles displayed a much stronger burst release at 20% compared to the particles containing immune potentiators. CpG and OVA are highly water-soluble molecules; meanwhile, our tested immune potentiators are more hydrophobic. One factor that contributes to burst release is the hydrophilicity, as formulations containing hydrophobic small molecules have been previously shown to dampen this effect.[19,20] The addition of immune potentiators may have assisted in dampening the burst release.

After observing promising loading and in vitro release data, the focus was shifted toward in vivo testing of the sustained-release potentiation. However, with the loading of up to three different components within a particle, there needed to be a strong consideration for the balance of antigen, agonist, and potentiator to ensure an accurate comparison between groups. In formulating particles, it is very difficult to standardize the concentration of two components across multiple formulations. Previous studies on antigen sparing have reported that the amount of adjuvant contributes more than the amount of antigen, especially at low antigen concentrations.[21−23] Therefore, we decided that when standardizing a concentration for the particles the adjuvant, CpG, would be kept standard across injections.

With the appropriate formulations ready, a series of vaccination experiments were conducted to test how potentiator particles would perform. To compare the effects of the controlled-release mechanism, formulations containing the same concentration of payload in solution without the presence of PLGA were included as control groups in the study and referred to as unencapsulated (Unen) (Table S2). There were no significant levels of CD8/OVA$^{257-264}$Tetramer+ cells measured, with all experimental groups having levels similar to


https://doi.org/10.1021/acsomega.3c06552
ACS Omega 2024, 9, 11608−11614

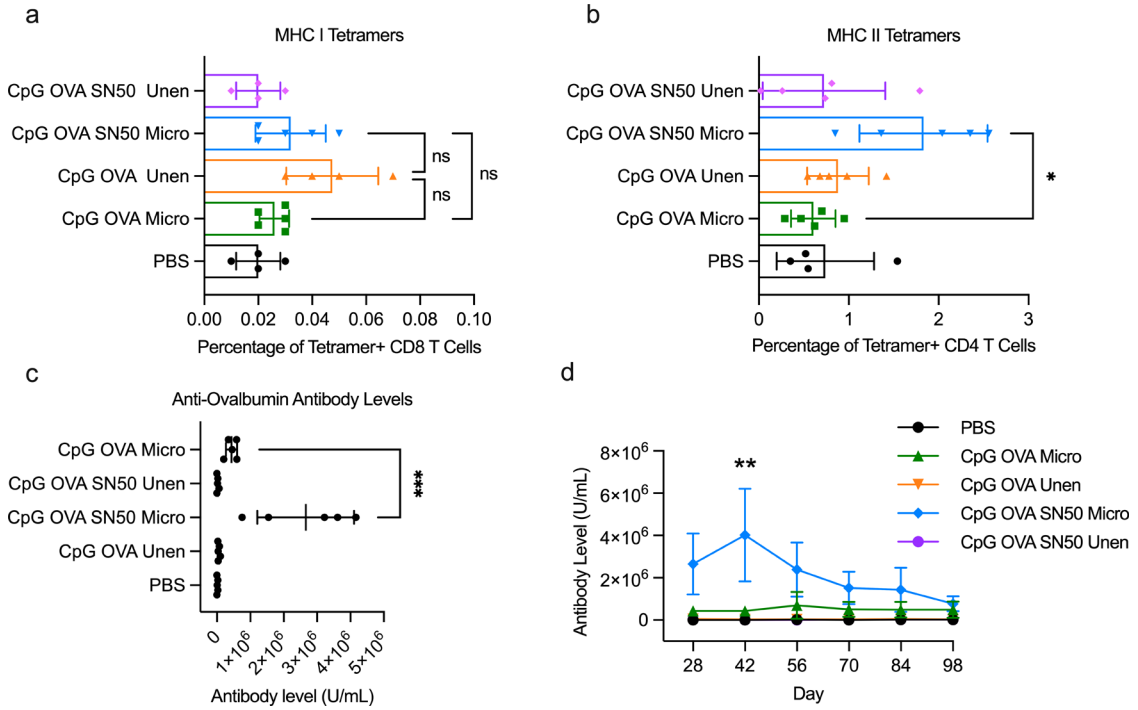


**Figure 2.** In vivo T-cell and antibody responses of controlled-release subunit vaccine containing SN50. (A) OVA-specific CD8 T-Cell responses measured by $OVA^{257-264}$MHC I from PBS (black bars), CpG OVA microparticles (green bars), CpG OVA unencapsulated (yellow bars), CpG OVA SN50 microparticles (blue bars), CpG OVA SN50 unencapsulated (purple bars). (B) OVA-specific CD4 T-Cell responses measured by $OVA^{323-339}$MHC II tetramers staining performed on lymphocytes harvested on day 21 ($n$ = 5). Some samples were not present due to not harvesting enough lymphocytes for staining. (C) Serum day 28 anti-ovalbumin Ig's (IgG + IgM + IgA) antibody levels measured from day 28 ($n$ = 5). (D) Anti-ovalbumin Ig's (IgG + IgM + IgA) antibody levels PBS (black), CpG OVA microparticles (green), CpG OVA Unencapsulated (yellow), CpG OVA SN50 Microparticles (blue), CpG OVA SN50 unencapsulated (purple) were measured over time from serum collected every 2 weeks after day 28 ($n$ = 5), mean reported with standard deviation as the error. Statistics was performed with unpaired $t$ test between CpG OVA Micro and CpG OVA SN50 Micro. One-way ANOVA was performed with Tukey's test. *$P$ < 0.05, **$P$ < 0.01, and ***$P$ < 0.001. Significance compared to CpG OVA microparticles. n.s., not significant.

those observed in the PBS control group (Figure 2A). The lack of $CD8/OVA^{257-264}$Tetramer+ cells suggests that none of the formulations promoted the growth of antigen-specific cytotoxic T cells, a hallmark of Th1-biased vaccine profiles. However, microparticles containing SN50 (CpG OVA SN50 Micro) had significantly higher $CD4/OVA^{323-339}$Tetramer+ staining than microparticles containing no immune potentiator (CpG OVA Micro) (Figure 2B).

The $CD4/OVA^{323-339}$Tetramer+ staining indicated a more robust MHC-II response, characteristic of Th2 immunity, in the presence of the SN50 immune potentiator particle vaccines. In contrast to Th1, Th2-biased immunity generates a strong humoral response and is effective against extracellular pathogens such as parasites and large microbes.[24] The Th2 response was further substantiated by the strong antibody levels exhibited by the immune potentiator particle vaccine, which was 6 times greater than the CpG OVA microparticle vaccine (Figure 2C). High IgG1-to-IgG2c ratios within serum samples are also characteristic of Th2 immunity.[25,26] CpG OVA SN50 particle's day 28 serum had a substantial IgG1-to-IgG2c ratio of 32 (Figure S1). This ratio was nearly 3 times higher than the CpG OVA microparticles, showcasing that SN50 further promoted an existing strong Th2 bias within the CpG OVA microparticle vaccine.

The strong Th2 biasing was initially surprising given that CpG is well documented to induce a Th1 response when formulated in solution, including in PLGA microparticle formulations.[27−30] However, some studies have reported that controlled-release PLGA particle vaccines containing CpG can dampen CpG's Th1 profile. Roman and co-workers co-formulated CpG and OVA microparticles with either PLGA 502 (ester-terminated, lactide/glycolide 50:50, $M_w$ 12 kDa) or PLGA 756 (ester-terminated, lactide/glycolide 75:25, $M_w$ 98 kDa). In vivo, the microparticle vaccines generated an IgG2a/IgG1 ratio of 0.50, compared to the 0.90 ratio for the CPG OVA solution formulation. Unlike the PLGA 502 microparticles, the PLGA 756's ex vivo-stimulated splenocytes generated no detectable IFN-$\gamma$ cytokine levels but were positive for IL-4.[31] Thus, this dampening effect seems to be dependent on the type of PLGA used. The size of PLGA microparticles also impacts CpG's immunogenicity, where larger particles above 1 $\mu$m have less Th1 bias compared to smaller microparticle formulations.[32] This phenomenon may be explained by the fact that the higher-molecular weight PLGA particles degrade slower than lower-molecular weight particles.[33,34] PLGA particles above 1 $\mu$m are less likely to be endocytosed and degrade extracellularly, thereby further promoting slow, steady release of CpG over time.[35,36] Both parameters allow less CpG to be available at once, subsequently decreasing CpG's immunogenicity effects in vivo. Based on the PLGA composition and size used in this study (ester-terminated, lactide: glycolide 50:50, $M_w$ 38−54 kDa), the particles strongly contributed to the Th2 bias, as typically seen with CpG-containing vaccine.

Overall, high antibody levels peaked at day 56 for the CpG OVA SN50 microparticles, and these antibody levels persisted


https://doi.org/10.1021/acsomega.3c06552
ACS Omega 2024, 9, 11608−11614

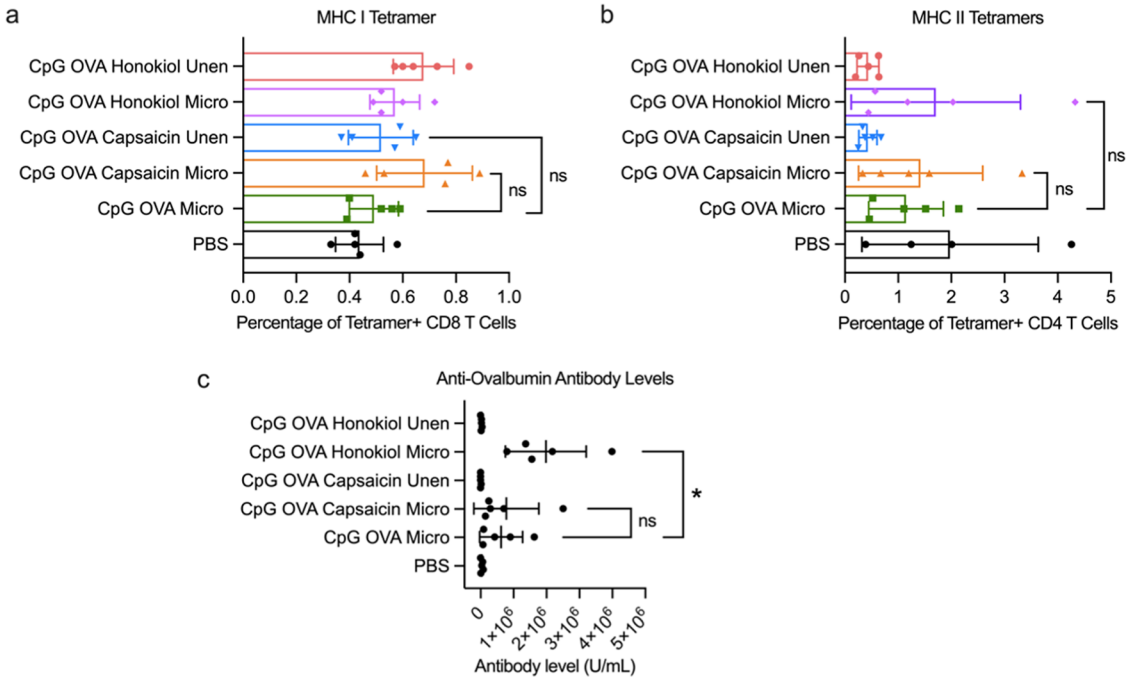


**Figure 3.** In vivo performance of controlled-release subunit vaccine containing capsaicin and honokiol. (A) Percentage of $OVA^{257-264}$ MHC I positive tetramer staining from PBS (black bars), CpG OVA microparticles (green bars), CpG OVA Capsaicin microparticle (yellow bars), CpG OVA Capsaicin unencapsulated (blue bars), CpG OVA Honokiol microparticles (purple bars), CpG OVA Honokiol unencapsulated (red bars). (B) $OVA^{323-339}$MHC II positive tetramers staining on lymphocytes ($n$ = 5). A few samples resulted in an insufficient number of lymphocytes for staining. (C) Day 28 anti-ovalbumin Ig's (IgG + IgM + IgA) antibody levels measured from day 28 serum ($n$ = 5). Mean reported with standard deviation as the error. One-way ANOVA was performed with Tukey's test. *$P$ < 0.05, **$P$ < 0.01, and ***$P$ < 0.001. n.s., not significant.

at higher levels for the entirety of the measured 98 days than the unencapsulated formulations. However, large variability within CpG OVA SN50 microparticles made the antibody levels lack statistical significance compared to CpG OVA microparticles beyond day 56 (Figure 2D).

Given the success of microparticles containing SN50, we next explored the efficacy of small-molecule immune potentiator microparticles in vivo. Previously, our group reported that honokiol and capsaicin were similar to SN50 in that they successfully suppressed systemic cytokines generated by subunit vaccines containing CpG while improving antibody levels.[9] Identical to the in vivo experiment with SN50-containing particles, honokiol and capsaicin particles were injected using the same route, volume, and balance of particles (Table S3).

Upon examination, in parallel to the SN50 experiment, $CD8/OVA^{257-264}$Tetramer+ levels showed that capsaicin and honokiol did not significantly improve T-cell activity compared to the CpG OVA microparticle formulation (Figure 3A). The same outcome was observed for $CD4/OVA^{323-339}$Tetramer+ staining, where no significant tetramers were observed (Figure 3B). While tetramer data was not substantial for antigen-specific CD4+ and CD8+ T cells, honokiol and capsaicin microparticles showed increased antibody levels on day 28 (Figure 3C). However, CpG OVA Honokiol microparticles were the only group significantly higher than the CpG OVA microparticles. Despite not observing significant MHCII tetramers, IgG subclasses showed an exceptionally high IgG1-to-IgG2c ratio of over 100 for both honokiol- and capsaicin-containing microparticles (Figure S2). The IgG1-to-IgG2c ratio was 10-fold higher than the CpG OVA microparticles. As demonstrated for the CpG OVA SN50 microparticles, the suppression of Th1 immunity most likely stems from the high-molecular weight polymer used and the size of the particles that is further enhanced by the immune potentiators. However, more mechanistic studies are needed to fully explain this process. Overall, the capsaicin and honokiol particle results suggest that improving CpG OVA microparticles may depend highly on the immune potentiator selected.

## CONCLUSIONS

In conclusion, we examined how immune potentiators alter and improve sustained-release vaccine formulations. SN50 microparticle formulations improved adjuvanted subunit microparticle vaccines by increasing antibody levels. We present evidence that particle formulation increased CD4/MHC-II-mediated antigen presentation. This increased response generally worked for both the peptide potentiator, SN50, and the small molecular potentiator, honokiol. The potentiators increased the absolute level of antibodies produced, up to 6-fold. They also increased the persistence of antibody levels—implying this could improve durability. Overall, these immune potentiator particle vaccines display a robust humoral response. While this approach may work best with certain vaccination strategies, it should be noted that the potentiators appear to amplify the preexisting outcomes of increased persistence and antibody response, which are hallmarks of particle-based vaccines. This study shows that potentiators can be used in particle formulations and that they enhance the existing immune activity of particle formulation without altering any underlying immune response.



https://doi.org/10.1021/acsomega.3c06552
ACS Omega 2024, 9, 11608−11614

## MATERIALS AND METHODS

**Materials.** Poly(lactic coglycolic acid) 50:50 (0.45−0.60 dL/g, $M_W$ = 38,000−54 000 Da, ester-terminated) and poly(vinyl alcohol) (87−89% hydrolyzed $M_W$ = 13,000−23,000) were purchased from Milipore-Sigma. CpG 1826 was created with a thioester backbone and purchased from Integrated DNA Technologies. Purified ovalbumin was purchased from Worthington Biomedical. Honokiol was obtained from TCI Chemicals (Japan), and capsaicin was purchased from Millipore Sigma. SN50 was created using a Liberty Blue peptide synthesizer and purified via HPLC. All other materials and assays were purchased from commercial sources.

**Particles Synthesis.** PLGA microspheres were formed using the double emulsion technique. Within a 1.5 mL Eppendorf tube, each individual payload was dissolved in 300 μL of phosphate-buffered saline (PBS) and then combined to a total volume of 900 μL. To ensure a comparable amount of CpG 1826 would be loaded in each particle, we measured the amount of CpG loading and then developed a molar ratio of components for loading. In the CpG/ovalbumin (OVA)/potentiator particles, the loading ratio was 5:7:55 with a starting concentration of 0.25 mM CpG in the aqueous layer. In the CpG/OVA particles, the ratio was 1:1 at 0.18 mM (see the SI for complete details). The contents of the Eppendorf tube were transferred to 2 mL of 100 mg/mL of PLGA in methylene chloride in a 20 mL glass scintillation vial. The mixture was ultrasonicated using an ultrasonic processer (Cole Parmer, 500 W) at 40% amplitude for 3 min (30 s stirring following 30 s of rest). After ultrasonification, 8 mL of 5% (w/v) PVA solution was added to the primary w/o emulsion and vortexed for 30 s to produce the w/o/w double emulsion. The w/o/w emulsion was poured into 180 mL of chilled 1% (w/v) PVA in a 400 mL beaker and stirred at room temperature for 6 h. The microspheres were centrifuged, and the pellet was washed three times with ultrapure deionized water and then lyophilized (Console Freeze-Dryer 6L, Labconco).

**Scanning Electron Microscopy.** Lyophilized particles were lightly dusted on an aluminum specimen stub with carbon tape. The particles were sputter coated with 10 nm of Pt/Pd (Cressington 208HR, Ted Pella) and then imaged on a high-resolution field emission scanning electron microscope (Merlin, Carl Zeis, Germany) at 3.0 kV for shape and morphology analysis.

**Loading Analysis.** Loading analysis was performed in triplicate using a previously reported extraction method.[12] In brief, 10 mg of particles were dissolved in 500 μL of dichloromethane and agitated for 30 min at 500 rpm on a plate shaker. Afterward, 250 μL of 0.1% sodium dodecyl sulfate in PBS was added to the dichloromethane layer and vortexed for 30 s. The layers were separated by centrifuging (15 min at 5000 rpm) and the top aqueous layer was collected. Extraction was performed again resulting in a total volume of 500 μL aqueous solution. The aqueous solution was either immediately evaluated or stored at −20 °C for later analysis. CpG and immune potentiator concentrations were measured on reverse-phase high-performance liquid chromatography (HPLC) via a standard curve. The method used a 0.6 mL/min flow rate with a C4 Jupiter column, 250 mm × 10 mm internal diameter, 10 μm particle size (Phenomenex). HPLC conditions for CpG included a 5 μL injection and an isocratic elution of 50% mobile phase of 0.1 M triethylammonium acetate buffer (solvent A) and 50% acetonitrile (solvent B). The CpG peak was detected at 254 nm with a linear concentration range of 20−200 μg/mL and an $R^2$ value of 0.9998. The immune potentiator method was conducted with a 20 μL injection and using a 20−80% gradient with 0.1% TFA water (solvent A) and 0.1% TFA acetonitrile. SN50 peak was observed at 212 nm and honokiol and capsaicin peak was observed at 254 nm (125−1000 μg/mL linear concentration range with $R^2$ = 0.9884, 0.2−1.9 μg/mL linear concentration range with $R^2$ = 0.9972, and 12.5−200 μg/mL linear concentration range with $R^2$ = 0. 9988, respectively) Protein and peptide levels were calculated using Qubit protein assay (Thermo Fisher) and evaluated on a Qubit Fluorometer (Thermo Fisher).

**In Vitro Release.** Gram vials containing 2 mg of OVA-loaded particles were treated with 0.5 mL of pH 7.45 PBS. The vials were gently stirred at 200 rpm at 37 °C. The particle solution was collected by centrifuging the vials at 4000 rpm for 10 min and stored at −20 °C. The OVA concentration was determined by using a Qubit Protein Assay (Thermo Fisher).

**Vaccination.** For the OVA experiments, ($n$ = 10) 6−8 week C57BL/6 mice (Jackson Laboratory) were lightly anesthetized with isoflurane. Particle formulations were injected to keep the amount of agonist, CpG, the same across groups. For injections where additional PLGA mass was required, empty microparticles composed only of PLGA (Table S2) were injected to keep the overall amount of injected PLGA the same between groups. Next, the mice were injected subcutaneously in the right flank with the appropriate amount of particles in 150 μL of PBS. Unencapsulated injections were formulated to the concentration of payload in the particle injections. Boost injections were provided on day 14, and on day 21, five mice were sacrificed for T-cell analysis.

**Serum Antibody Levels.** Cheek bleeds were collected on days 28, 42, 56, 70, 84, and 98. Samples were clotted for 30 min at room temperature before being centrifuged at 2000$g$ for 10 min. The supernatants were collected and stored at −80 °C until testing. An α Diagnostic International mouse anti-ovalbumin (Gal d 2) Ig's (IgG, IgA, IgM) ELISA Kit, 96 tests were used following the manufacturer's instructions to quantify the serum's antibody titer. Anti-ovalbumin IgG1, IgG2c, IgG3, and IgG2b levels were determined via quantitative ELISA (α Diagnostic International) on day 28 serum by following the manufacturer's protocol. Serum was diluted using the manufacturer's diluent. The antibody levels were quantified from the standard curve from known concentrations provided in the kit.

**T-Cell Response.** Murine lymphocytes from the radial, auxiliary, and inguinal lymph nodes were harvested on day 21. Lymph nodes were treated with 500 μL of 5 mg/mL collagenase-d in RPMI media for 30 min in a cell incubator (37 °C) before being mashed with a syringe plunger. The lymphocytes were vigorously pipetted to a single-cell suspension. The lymphocytes were washed with RPMI and resuspended in T-cell media. The lymphocytes were counted on a hemocytometer, and 1 million cells from each sample were plated on two 96-well plates. For each tetramer staining (MBL International), the $OVA_{323-339}$ and $OVA_{257-264}$ tetramer staining was conducted according to the manufacturer's protocol. For the MHCI tetramer, cells were treated with Fc block before tetramer staining. The sample was washed twice with 100 μL of FACS (2% FBS in PBS) buffer and then treated with 10 μL of tetramer solution. Afterward, the sample was left to incubate in the dark for 30 min at room temperature. The


https://doi.org/10.1021/acsomega.3c06552
ACS Omega 2024, 9, 11608−11614

plate was washed with FACS buffer and then treated with FITC-labeled anti-CD8 antibody (Biolegend) and live dead stain (Thermo Fisher). The samples were incubated for 30 min at room temperature and then washed with FACS buffer three times. The cells were resuspended in FACS buffer before being processed using flow cytometry (ACEA NovoCyte Agilent Technologies). MHCII tetramer staining was performed similarly with FITC-labeled anti-CD4 antibody (Biolegend); however, the cells were incubated with 10 $\mu$g/mL $OVA_{323-339}$ and 0.5 ng/mL IL-2 for 6 days for performing the staining protocol.

**Statistical Analysis.** Statistical analyses were carried out using GraphPad Prism 9.0 software. One-way ANOVA with Tukey's test was used to compare the experimental groups with one another or unpaired *t* test to compare two groups with one another. Values are reported as mean ± SD (standard deviation). Significance $^{*}P < 0.05$, $^{**}P < 0.01$, $^{***}P < 0.001$, and $^{****}P < 0.0001$. n.s., not significant

## ■ ASSOCIATED CONTENT

### Supporting Information

The Supporting Information is available free of charge at https://pubs.acs.org/doi/10.1021/acsomega.3c06552.

Details on encapsulation efficiency, amount of particles injected, anti-OVA IgG subclass results, and an example of the tetramer gating strategy (PDF)

## ■ AUTHOR INFORMATION


### Corresponding Author

**Aaron P. Esser- Kahn** − *Pritzker School of Molecular Engineering, University of Chicago, Chicago, Illinois 60637, United States;* orcid.org/0000-0003-1273-0951; Email: aesserkahn@uchicago.edu

### Authors

**Britteny J. Cassaidy** − *Pritzker School of Molecular Engineering, University of Chicago, Chicago, Illinois 60637, United States*

**Brittany A. Moser** − *Pritzker School of Molecular Engineering, University of Chicago, Chicago, Illinois 60637, United States*

**Ani Solanki** − *Animal Resource Center, University of Chicago, Chicago, Illinois 60637, United States*

**Qing Chen** − *Pritzker School of Molecular Engineering, University of Chicago, Chicago, Illinois 60637, United States*

**Jingjing Shen** − *Pritzker School of Molecular Engineering, University of Chicago, Chicago, Illinois 60637, United States*

**Kristen Gotsis** − *Pritzker School of Molecular Engineering, University of Chicago, Chicago, Illinois 60637, United States*

**Zoe Lockhart** − *Pritzker School of Molecular Engineering, University of Chicago, Chicago, Illinois 60637, United States*

**Nakisha Rutledge** − *Pritzker School of Molecular Engineering, University of Chicago, Chicago, Illinois 60637, United States*

**Matthew G. Rosenberger** − *Pritzker School of Molecular Engineering, University of Chicago, Chicago, Illinois 60637, United States;* orcid.org/0000-0002-0595-5338

**Yixiao Dong** − *Pritzker School of Molecular Engineering, University of Chicago, Chicago, Illinois 60637, United States*

**Delaney Davis** − *Pritzker School of Molecular Engineering, University of Chicago, Chicago, Illinois 60637, United States*

Complete contact information is available at: https://pubs.acs.org/10.1021/acsomega.3c06552


### Notes

The authors declare no competing financial interest.

## ■ ACKNOWLEDGMENTS

All of the authors contributed equally to this work. The authors thank Marie Kim for particle analysis assistance. They also thank Dr. Justin Jureller, MRSEC facility, University of Chicago, for SEM assistance. This work was supported by a grant from DTRA (HDTRA11810052).

## ■ REFERENCES


(1) Allahyari, M.; Mohit, E. Peptide/Protein Vaccine Delivery System Based on PLGA Particles. *Hum. Vaccines Immunother.* **2016**, *12* (3), 806−828.

(2) Nie, T.; Wang, W.; Liu, X.; Wang, Y.; Li, K.; Song, X.; Zhang, J.; Yu, L.; He, Z. Sustained Release Systems for Delivery of Therapeutic Peptide/Protein. *Biomacromolecules* **2021**, *22* (6), 2299−2324.

(3) Higuchi, T. Mechanism of Sustained-action Medication. Theoretical Analysis of Rate of Release of Solid Drugs Dispersed in Solid Matrices. *J. Pharm. Sci.* **1963**, *52* (12), 1145−1149.

(4) Kanchan, V.; Panda, A. K. Interactions of Antigen-Loaded Polylactide Particles with Macrophages and Their Correlation with the Immune Response. *Biomaterials* **2007**, *28* (35), 5344−5357.

(5) Fu, Y.; Kao, W. J. Drug Release Kinetics and Transport Mechanisms of Non-Degradable and Degradable Polymeric Delivery Systems. *Expert Opin. Drug Delivery* **2010**, *7* (4), 429−444.

(6) Koerner, J.; Horvath, D.; Groettrup, M. Harnessing Dendritic Cells for Poly (D,L-Lactide-Co-Glycolide) Microspheres (PLGA MS)—Mediated Anti-Tumor Therapy. *Front. Immunol.* **2019**, *10*, No. 707, DOI: 10.3389/fimmu.2019.00707.

(7) Lin, Y.-Z.; Yao, S.; Veach, R. A.; Torgerson, T. R.; Hawiger, J. Inhibition of Nuclear Translocation of Transcription Factor NF-κB by a Synthetic Peptide Containing a Cell Membrane-Permeable Motif and Nuclear Localization Sequence. *J. Biol. Chem.* **1995**, *270* (24), 14255−14258, DOI: 10.1074/jbc.270.24.14255.

(8) Moser, B. A.; Steinhardt, R. C.; Escalante-Buendia, Y.; Boltz, D. A.; Barker, K. M.; Cassaidy, B. J.; Rosenberger, M. G.; Yoo, S.; McGonnigal, B. G.; Esser-Kahn, A. P. Increased Vaccine Tolerability and Protection via NF-κB Modulation. *Sci. Adv.* **2020**, *6* (37), No. eaaz8700.

(9) Moser, B. A.; Escalante-Buendia, Y.; Steinhardt, R. C.; Rosenberger, M. G.; Cassaidy, B. J.; Naorem, N.; Chon, A. C.; Nguyen, M. H.; Tran, N. T.; Esser-Kahn, A. P. Small Molecule NF-κB Inhibitors as Immune Potentiators for Enhancement of Vaccine Adjuvants. *Front. Immunol.* **2020**, *11*, No. 511513.

(10) Kobayashi, A.; Osaka, T.; Namba, Y.; Inoue, S.; Lee, T. H.; Kimura, S. Capsaicin Activates Heat Loss and Heat Production Simultaneously and Independently in Rats. *Am. J. Physiol.: Regul., Integr. Comp. Physiol.* **1998**, *275* (1), R92−R98.

(11) Bailey, B. A.; Ochyl, L. J.; Schwendeman, S. P.; Moon, J. J. Toward a Single-Dose Vaccination Strategy with Self-Encapsulating PLGA Microspheres. *Adv. Healthcare Mater.* **2017**, *6* (12), No. 1601418.

(12) Saez, V.; Ramón, J. A.; Caballero, L.; Aldana, R.; Cruz, E.; Peniche, C.; Paez, R. Extraction of PLGA-Microencapsulated Proteins Using a Two-Immiscible Liquid Phases System Containing Surfactants. *Pharm. Res.* **2013**, *30* (2), 606−615.

(13) Shen, H.; Ackerman, A. L.; Cody, V.; Giodini, A.; Hinson, E. R.; Cresswell, P.; Edelson, R. L.; Saltzman, W. M.; Hanlon, D. J. Enhanced and Prolonged Cross-Presentation Following Endosomal Escape of Exogenous Antigens Encapsulated in Biodegradable Nanoparticles. *Immunology* **2006**, *117* (1), 78−88.

(14) Hamdy, S.; Haddadi, A.; Hung, R. W.; Lavasanifar, A. Targeting Dendritic Cells with Nano-Particulate PLGA Cancer Vaccine Formulations. *Adv. Drug Delivery Rev.* **2011**, *63* (10−11), 943−955.

(15) Chua, B. Y.; Sekiya, T.; Al Kobaisi, M.; Short, K. R.; Mainwaring, D. E.; Jackson, D. C. A Single Dose Biodegradable

Vaccine Depot That Induces Persistently High Levels of Antibody over a Year. *Biomaterials* **2015**, *53*, 50−57.
(16) Sharma, A.; Vaghasiya, K.; Verma, R. K. Inhalable Microspheres with Hierarchical Pore Size for Tuning the Release of Biotherapeutics in Lungs. *Microporous Mesoporous Mater.* **2016**, *235*, 195−203.
(17) Si, W.; Yang, Q.; Zong, Y.; Ren, G.; Zhao, L.; Hong, M.; Xin, Z. Toward Understanding the Effect of Solvent Evaporation on the Morphology of PLGA Microspheres by Double Emulsion Method. *Ind. Eng. Chem. Res.* **2021**, *60* (25), 9196−9205.
(18) D'Souza, S. S.; DeLuca, P. P. Methods to Assess in Vitro Drug Release from Injectable Polymeric Particulate Systems. *Pharm. Res.* **2006**, *23* (3), 460−474.
(19) Yoo, J.; Won, Y.-Y. Phenomenology of the Initial Burst Release of Drugs from PLGA Microparticles. *ACS Biomater. Sci. Eng.* **2020**, *6* (11), 6053−6062.
(20) Horvath, D.; Basler, M. PLGA Particles in Immunotherapy. *Pharmaceutics* **2023**, *15* (2), No. 615, DOI: 10.3390/pharmaceutics15020615.
(21) Reisinger, K. S.; Holmes, S. J.; Pedotti, P.; Arora, A. K.; Lattanzi, M. A Dose-Ranging Study of MF59 -Adjuvanted and Non-Adjuvanted A/H1N1 Pandemic Influenza Vaccine in Young to Middle-Aged and Older Adult Populations to Assess Safety, Immunogenicity, and Antibody Persistence One Year after Vaccination. *Hum. Vaccines Immunother.* **2014**, *10* (8), 2395−2407.
(22) Jiang, J.; Fisher, E. M.; Hensley, S. E.; Lustigman, S.; Murasko, D. M.; Shen, H. Antigen Sparing and Enhanced Protection Using a Novel rOv-ASP-1 Adjuvant in Aqueous Formulation with Influenza Vaccines. *Vaccine* **2014**, *32* (23), 2696−2702.
(23) Kuo, T.-Y.; Lin, M.-Y.; Coffman, R. L.; Campbell, J. D.; Traquina, P.; Lin, Y.-J.; Liu, L. T.-C.; Cheng, J.; Wu, Y.-C.; Wu, C.-C.; Tang, W.-H.; Huang, C.-G.; Tsao, K.-C.; Chen, C. Development of CpG-Adjuvanted Stable Prefusion SARS-CoV-2 Spike Antigen as a Subunit Vaccine against COVID-19. *Sci. Rep* **2020**, *10* (1), No. 20085.
(24) Walker, J. A.; McKenzie, A. N. J. TH2 Cell Development and Function. *Nat. Rev. Immunol.* **2018**, *18* (2), 121−133.
(25) Nazeri, S.; Zakeri, S.; Mehrizi, A. A.; Sardari, S.; Djadid, N. D. Measuring of IgG2c Isotype Instead of IgG2a in Immunized C57BL/6 Mice with Plasmodium Vivax TRAP as a Subunit Vaccine Candidate in Order to Correct Interpretation of Th1 versus Th2 Immune Response. *Exp. Parasitol.* **2020**, *216*, No. 107944.
(26) Halliday, A.; Turner, J. D.; Guimarães, A.; Bates, P. A.; Taylor, M. J. The TLR2/6 Ligand PAM2CSK4 Is a Th2 Polarizing Adjuvant in Leishmania Major and Brugia Malayi Murine Vaccine Models. *Parasites Vectors* **2016**, *9* (1), No. 96, DOI: 10.1186/s13071-016-1381-0.
(27) Chu, R. S.; Targoni, O. S.; Krieg, A. M.; Lehmann, P. V.; Harding, C. V. CpG Oligodeoxynucleotides Act as Adjuvants That Switch on T Helper 1 (Th1) Immunity. *J. Exp. Med.* **1997**, *186* (10), 1623−1631.
(28) Millan, C. L. B.; Weeratna, R.; Krieg, A. M.; Siegrist, C.-A.; Davis, H. L. CpG DNA Can Induce Strong Th1 Humoral and Cell-Mediated Immune Responses against Hepatitis B Surface Antigen in Young Mice. *Proc. Natl. Acad. Sci. U.S.A.* **1998**, *95* (26), 15553−15558.
(29) Krieg, A. M. Immune Effects and Mechanisms of Action of CpG Motifs. *Vaccine* **2000**, *19* (6), 618−622.
(30) Wang, Q.; Tan, M. T.; Keegan, B. P.; Barry, M. A.; Heffernan, M. J. Time Course Study of the Antigen-Specific Immune Response to a PLGA Microparticle Vaccine Formulation. *Biomaterials* **2014**, *35* (29), 8385−8393.
(31) Román, B. S.; Gómez, S.; Irache, J. M.; Espuelas, S. Co-Encapsulated CpG Oligodeoxynucleotides and Ovalbumin in PLGA Microparticles; An in Vitro and in Vivo Study. *J. Pharm. Pharm. Sci.* **2014**, *17* (4), No. 541, DOI: 10.18433/J33892.
(32) Joshi, V. B.; Geary, S. M.; Salem, A. K. Biodegradable Particles as Vaccine Delivery Systems: Size Matters. *AAPS J.* **2013**, *15* (1), 85−94.
(33) Makadia, H. K.; Siegel, S. J. Poly Lactic-Co-Glycolic Acid (PLGA) as Biodegradable Controlled Drug Delivery Carrier. *Polymers* **2011**, *3* (3), 1377−1397.
(34) Kumskova, N.; Ermolenko, Y.; Osipova, N.; Semyonkin, A.; Kildeeva, N.; Gorshkova, M.; Kovalskii, A.; Kovshova, T.; Tarasov, V.; Kreuter, J.; Maksimenko, O.; Gelperina, S. How Subtle Differences in Polymer Molecular Weight Affect Doxorubicin-Loaded PLGA Nanoparticles Degradation and Drug Release. *J. Microencapsulation* **2020**, *37* (3), 283−295.
(35) Desai, M. P.; Labhasetwar, V.; Walter, E.; Levy, R. J.; Amidon, G. L. The Mechanism of Uptake of Biodegradable Microparticles in Caco-2 Cells Is Size Dependent. *Pharm. Res.* **1997**, *14* (11), 1568−1573.
(36) De Almeida, M. S.; Susnik, E.; Drasler, B.; Taladriz-Blanco, P.; Petri-Fink, A.; Rothen-Rutishauser, B. Understanding Nanoparticle Endocytosis to Improve Targeting Strategies in Nanomedicine. *Chem. Soc. Rev.* **2021**, *50* (9), 5397−5434.


https://doi.org/10.1021/acsomega.3c06552
*ACS Omega* 2024, 9, 11608−11614